

Möbius invariant Y-systems (cluster structures) for Miquel dynamics

Niklas C. Affolter

Institut für Mathematik, TU Berlin,
Straße des 17. Juni 136, 10623 Berlin, Germany

December 11, 2023

Abstract. Miquel dynamics is a discrete time dynamics for circle patterns. Previous work shows that the circle centers satisfy the dSKP equation on the octahedral lattice A_3 and give rise to a real-valued Y-system / cluster structure. In this article we show that half the intersection points satisfy the dSKP equation as well, and we introduce two new real-valued Y-systems for Miquel dynamics that involve only the intersection points. Therefore, the new Y-systems are Möbius invariant. We also show that the circle centers and intersection points combined satisfy the dSKP equation on the 4-dimensional octahedral lattice A_4 . In addition, we present two more complex-valued Y-systems for Miquel dynamics, which are real-valued in and only in the case of integrable circle patterns. We also show that in the case of harmonic embeddings, the old and the new Y-patterns coincide.

Contents

| | | |
|---|-------------------------------------|----|
| 1 | Introduction | 2 |
| 2 | Combinatorics of A_3 | 7 |
| 3 | Miquel maps | 8 |
| 4 | dSKP maps | 9 |
| 5 | Y-systems | 11 |
| 6 | Integrable circle patterns | 14 |
| 7 | A combined dSKP map on A_4 | 17 |
| 8 | Cluster algebras | 20 |
| 9 | X-variables for harmonic embeddings | 21 |

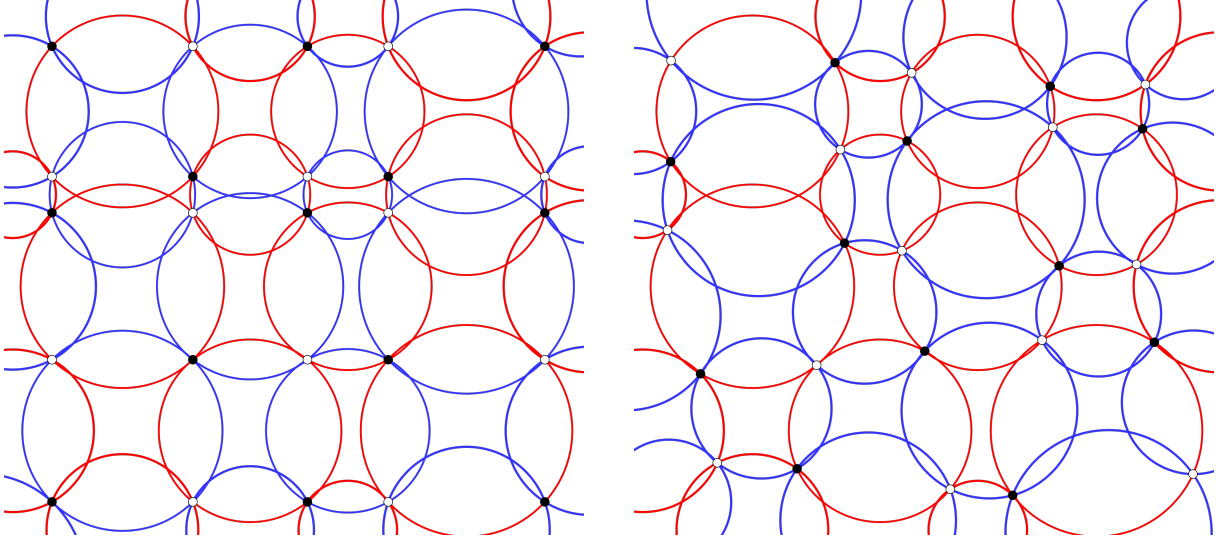


Figure 1. Miquel dynamics transforms the circle pattern (c_0, p_0) on the left into the circle pattern (c_1, p_1) on the right, by replacing all the blue circles.

1 Introduction

Let $F(\mathbb{Z}^2)$ denote the faces of \mathbb{Z}^2 , and let $\hat{\mathbb{C}} = \mathbb{C} \cup \{\infty\}$ denote the complex projective line.

Definition 1.1. A *circle pattern* (c, p) is a pair of maps

$$c : \mathbb{Z}^2 \rightarrow \text{Circles}(\hat{\mathbb{C}}), \quad (1.1)$$

$$p : F(\mathbb{Z}^2) \rightarrow \hat{\mathbb{C}}, \quad (1.2)$$

such that $p(v) \in c(f)$ whenever $v \in f$.

Miquel dynamics [Ram18] is a discrete time dynamics on circle patterns, and the evolution of Miquel dynamics produces a sequence of circle patterns $(c_k, p_k)_{k \in \mathbb{Z}}$, see also Figure 1. Let us explain how Miquel dynamics are defined, beginning with a circle pattern (c_0, p_0) . The vertices of \mathbb{Z}^2 may be partitioned into *even vertices* and *odd vertices*, where even and odd refer to the parity of the coordinate sum. Consider an even vertex $v \in V$ and its four adjacent vertices v_1, v_2, v_3, v_4 in counterclockwise order, see Figure 2. The circles $c_0(v_1)$ and $c_0(v_2)$ have one intersection point $p_0(f_{12})$ on $c_0(v)$, and generically they have a second intersection point $p_1(f_{12})$. The exception is if $c_0(v_1), c_0(v_2)$ are tangent, in which case we set $p_1(f_{12}) = p_0(f_{12})$. Throughout we assume it is understood that in the case of tangent circles the second or the other intersection point is the same as the first intersection point. *Miquel's theorem* [Miq38] states that the four points $p_1(f_{12}), p_1(f_{23}), p_1(f_{34}), p_1(f_{41})$ are on a circle, which we denote by $c_1(v)$. By setting $c_1(v) = c_0(v)$ for all odd vertices, we obtain a new circle pattern (c_1, p_1) . We say the two circle patterns are related by Miquel dynamics. Note that this operation is invertible by applying the same procedure to the even circles again. However, applying the substitution to all odd circles yields a new circle pattern (c_2, p_2) . Therefore, by alternating even and odd substitutions we obtain a bi-infinite sequence of circle patterns $(c_k, p_k)_{k \in \mathbb{Z}}$, which is the forwards and backwards evolution of Miquel dynamics.

Let us denote by $t : \mathbb{Z}^2 \rightarrow \mathbb{C}$ the circle centers of c . We call a map t that arises as the circle centers of a circle pattern a *conical net*, see for example [Mü15]. Conical nets

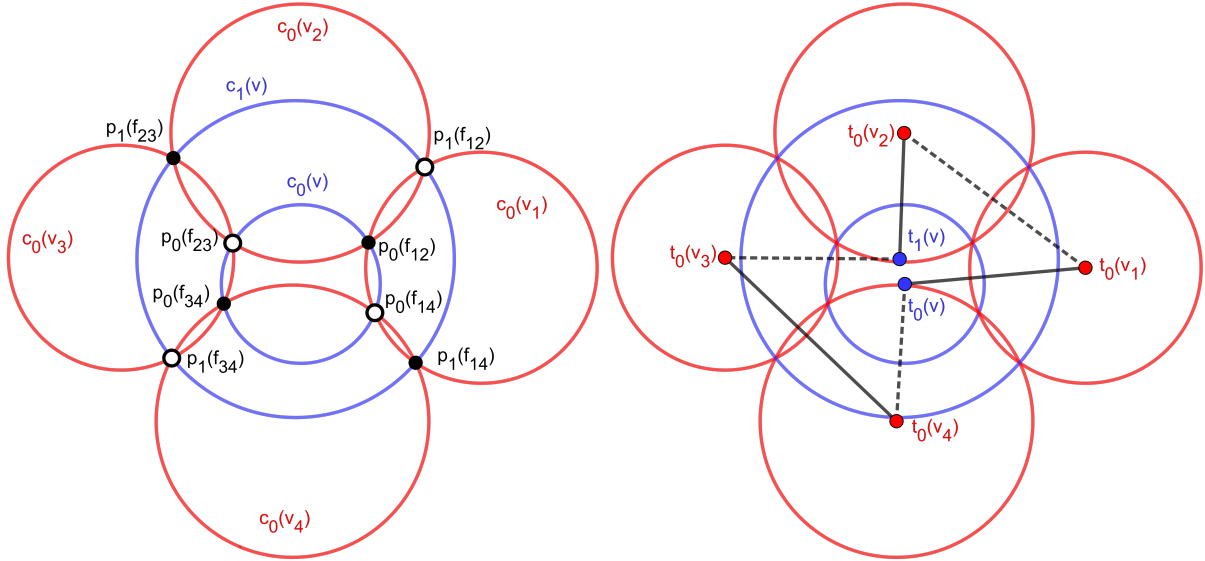


Figure 2. Local labeling in Miquel dynamics, Equation 1.4 is highlighted on the right.

are also called *Coloumb gauge* in [KLRR22] and *t-realization* in [CLR23]. A special case of *t-realizations* are *t-embeddings*, which are conical nets with an additional embedding property.

The *multi-ratio* of an even number of points $a_1, a_2, \dots, a_{2m} \in \hat{\mathbb{C}}$ is defined as

$$\text{mr}(a_1, a_2, \dots, a_{2m}) := \frac{(a_1 - a_2) \cdots (a_{2m-1} - a_{2m})}{(a_2 - a_3) \cdots (a_{2m} - a_1)}. \quad (1.3)$$

We assume throughout the paper that none of the circles of c_k contains the point at infinity, and therefore all the circle centers in t are indeed in \mathbb{C} .

The following equation was discovered in [Aff21] and independently in [KLRR22]

$$\text{mr}(t_k(v), t_k(v_1), t_k(v_2), t_{k+1}(v), t_k(v_3), t_k(v_4)) = -1, \quad (1.4)$$

where the labeling of the faces is as shown in Figure 2. This equation is Equation (χ_2) in the classification of integrable discrete equations of octahedron type [ABS12]. Indeed, Equation (1.4) posses the full symmetry of the octahedron, that is it is invariant under any cyclic permutation of the arguments and each argument swap $1 \leftrightarrow 4$, $2 \leftrightarrow 5$ and $3 \leftrightarrow 6$. As an equation on the octahedral lattice, Equation (1.4) is also known as the *dSKP equation*, studied in [KS02] but first discovered in [DN91, NCWQ84]. We will explain the octahedral lattice in more detail in Section 2, and the interpretation of Miquel dynamics on the octahedral lattice in Section 3.

Consider a conical net t_k and a vertex v such that the center $t_k(v)$ is being replaced by Miquel dynamics in t_{k+1} . Then we define the *Y-variables*

$$Y_k(v) = -\frac{(t_k(v_1) - t_k(v))(t_k(v_3) - t_k(v))}{(t_k(v_2) - t_k(v))(t_k(v_4) - t_k(v))}, \quad (1.5)$$

where the labels are as in Figure 2. It was shown in [Aff21, KLRR22] that Y is real-valued. Moreover, if t is a *t-embedding* then Y is necessarily positive as well.

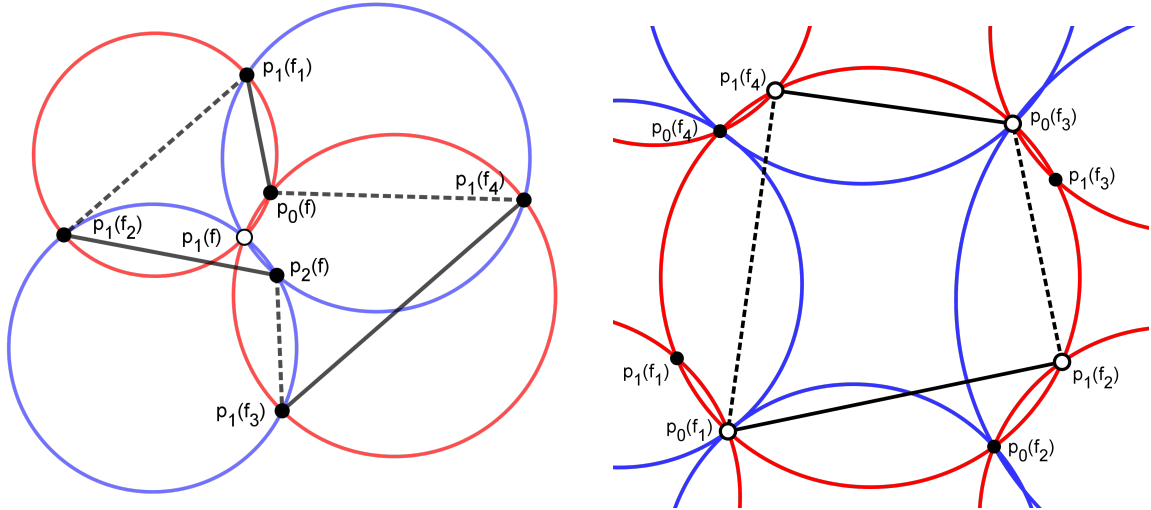


Figure 3. Left: a Clifford configuration, the red (blue) circles are part of c_0 and c_1 (c_1 and c_2). Right: the points that define the X° -variables, the red (blue) circles are part of c_0 and c_1 (c_{-1} and c_0).

Additionally, it was shown that the Y -variables together with Miquel dynamics constitute a Y -system (see [KNS11]), that is they satisfy

$$Y_{k+2}(v)Y_k(v) = \frac{(1 + Y_{k+1}(v_2))(1 + Y_{k+1}(v_4))}{(1 + Y_{k+1}^{-1}(v_1))(1 + Y_{k+1}^{-1}(v_3))}. \quad (1.6)$$

Note that we are using a convention for Y -systems where we substitute $Y \mapsto -Y$. With this convention, it is obvious that if an initial circle pattern has positive Y -variables, the Y -variables remain positive under Miquel dynamics. We explain this relation in more detail in Section 5. There is also an equivalent formulation, stating that the Y -variables behave as cluster variables do under *mutation* in a cluster algebra [FZ01], we briefly explain this relation in Section 8.

The first new result we present is that the dSKP equation does not only show up among the circle centers of a circle pattern, but also directly in the circle intersection point. Specifically, we show in Theorem 4.4 that

$$\text{mr}(p_{k-1}(f), p_k(f_1), p_k(f_2), p_{k+1}(f), p_k(f_3), p_k(f_4)) = -1, \quad (1.7)$$

where the labels are as in Figure 3 (left). Since $F(\mathbb{Z}^2) \simeq \mathbb{Z}^2$, the faces of \mathbb{Z}^2 may also be partitioned into even (parity) faces and odd (parity) faces. Let p_k^\bullet be the restriction of p_k to even faces if k is even and the restriction to odd faces if k is odd. Analogously, let p_k° be the restriction of p_k to odd faces if k is even and the restriction to even faces if k is odd. Equation (1.7) involves either only points of p^\bullet or only points of p° . As a result, both p^\bullet and p° solve the dSKP equation on the octahedral lattice, as we show in Section 4.

The multi-ratio $a_1, a_2, a_3, a_4 \in \hat{\mathbb{C}}$ of four points is called the *cross-ratio*

$$\text{cr}(a_1, a_2, a_3, a_4) = \text{mr}(a_1, a_2, a_3, a_4). \quad (1.8)$$

Consider a circle $c_k(f)$ that is not replaced in the next iteration of Miquel dynamics and the labeling in Figure 3 (right). We define the X^\bullet -variables and the X° -variables

$$X_k^\bullet(f) = -\text{cr}(p_k^\bullet(f_1), p_{k+1}^\bullet(f_2), p_k^\bullet(f_3), p_{k+1}^\bullet(f_4)), \quad (1.9)$$

$$X_k^\circ(f) = -\text{cr}(p_{k+1}^\circ(f_1), p_k^\circ(f_2), p_{k+1}^\circ(f_3), p_k^\circ(f_4)). \quad (1.10)$$

Since each $X_k(f)$ is the cross-ratio of four points on a circle, both the X^\bullet - and the X° -variables are real-valued. In Section 5 we show that both X^\bullet and X° constitute a Y-system. As a consequence, if the X -variables are positive initially, the positivity is also preserved by Miquel dynamics.

A Möbius transformation $M : \hat{\mathbb{C}} \rightarrow \hat{\mathbb{C}}$ is a transformation of the form

$$M(z) = \frac{az + b}{cz + d}, \quad (1.11)$$

for some $a, b, c, d \in \mathbb{C}$ with $ad \neq bc$. The definition of a circle pattern is invariant under Möbius transformations of $\hat{\mathbb{C}}$. However, the Möbius transformation of a conical net is not a conical net, conical nets are only invariant under similarity transformations of $\hat{\mathbb{C}}$. Nor are the Y -variables invariant under Möbius transformations. On the other hand, cross-ratios are invariant under Möbius transformations and therefore the X -variables are also invariant under Möbius transformations. Circle patterns are studied as discretizations of conformal maps. Since Möbius transformations are in a sense the “simplest” conformal maps, in *discrete differential geometry* (see [BS08]), one usually studies Möbius invariant quantities of circle patterns, like the intersection angles of circles or the cross-ratios of intersection points. In that sense, the X -variables are more suitable to the purposes of discrete differential geometry than the Y -variables are, and provide a link between discrete conformal theories and real-valued Y-systems and cluster algebras.

Consider the formulas (1.9) and (1.10) but at a face f that is replaced by the next iteration of Miquel dynamics. We call the resulting variables the W^\bullet - and W° -variables. In Section 6, we show that these variables are also Y-systems, but not real-valued ones. Interestingly, they do satisfy $W^\bullet = \bar{W}^\circ$, that is they are complex conjugates. Therefore if the W^\bullet -variables are real, then $W^\bullet = W^\circ$. We show that this special case of real W -variables corresponds to *integrable circle patterns*, which were introduced in [BMS05].

Remark 1.2. Note that with the Y -, X - and W -variables there are three *different* ways to obtain a Y-system for a dSKP map. The Y -variables are an *affine* notion (affine geometry of \mathbb{C}), the X - and W -variables are a *projective* notion (projective geometry of \mathbb{CP}^1), as explained in more detail in [Aff23]. It is also possible to associate projective variables to the conical net, and affine variables to the intersection points. However, in this case the resulting variables are not necessarily real-valued anymore, we give an overview in Table 1. The affine variables for a dSKP map were first considered in [Aff21, KLRR22], but they already appear as cluster variables already for *T-graphs* in [KS04], which are related to *Menelaus lattices* as defined in [KS02]. The projective variables for general dSKP maps are discussed in [ABS12], and coincide with the cluster variables for the pentagram map [Gli11].

There is a way to combine circle intersection points p and circle centers t that solves the dSKP equation on a higher-dimensional octahedral lattice, the A_4 lattice. This shows that from the dSKP perspective, (half) the intersection points are a Bäcklund transform of the circle centers and vice versa. In Section 7 we explain the combinatorics of A_4 and this result in more detail. It is beyond the scope of this paper, but in a similar vein one can show that if one adds additional boundary cluster variables to the Y -variables, the X -variables are related to these extended Y -variables by a sequence of cluster mutations, see [Aff23]. In particular, this suggests that the positivity of the X - and Y -variables may be more closely related than would be expected at first glance.

| | t -map | p^\bullet -map | p° -map |
|----------------|----------|---------------------|---------------------|
| Y -variables | real | complex | complex |
| X -variables | complex | real | real |
| W -variables | complex | real iff ICP | real iff ICP |

Table 1. Overview of the various Y -systems associated to Miquel dynamics, ICP is short for integrable circle pattern. In bold are the Y -systems that are invariant under Möbius transformations of the circle patterns.

For conical nets, in the language of t -embeddings, two special cases are of particular interest: t -embeddings associated to *harmonic embeddings* – which we call h -embeddings – and s -embeddings [Che18], see also [KLRR22] for both. In Section 9, we study h -embeddings with general quad-graph combinatorics. We explain how to introduce Möbius invariant X -variables for h -embeddings. Then we show that in h -embeddings, the X - and Y - variables *coincide*. This implies that there is a class of generalized h -embeddings which are Möbius invariant in the sense that we may apply Möbius transformations to the underlying circle pattern while preserving the X -variables. We leave it as an open question, whether there is also a special relation between X - and Y -variables in the case of s -embeddings.

Plan of the paper

In Section 2, we introduce the combinatorics of A_3 as viewed on \mathbb{Z}_+^3 , which we denote \mathcal{L} , and explain the occurrence of tetrahedra \mathcal{T} and octahedra \mathcal{O} in \mathcal{L} . In Section 3, we put the evolution of Miquel dynamics on the lattice \mathcal{L} , we call the resulting objects *Miquel maps*. In particular, we associated circles and centers with \mathcal{L} , and intersection points with the tetrahedra \mathcal{T} . In Section 4, we explain and prove the dSKP results for Miquel maps on \mathcal{L} . In Section 5, we explain the Y -system results for Y - and X -variables on \mathcal{L} . In Section 6, we introduce what we call *W-variables* for Miquel maps, which are also a Y -system, but a complex-valued one. We show that the special case of real W -variables is the case of so called *integrable circle patterns*. In Section 7, we show how to identify $\mathcal{T} \cup \mathcal{L}$ with a subset of A_4 . Then we prove that with this identification, the combined map of centers and intersection points solves the dSKP equation on A_4 . In Section 8, we briefly explain the relation of Y -patterns to cluster algebras. Finally, in Section 9 we show that X - and Y -variables coincide in the special case of h -embeddings.

Acknowledgments

The author is supported by the Deutsche Forschungsgemeinschaft (DFG) Collaborative Research Center TRR 109 “Discretization in Geometry and Dynamics”. I would like to thank Sanjay Ramassamy, Wolfgang Schief and Boris Springborn for discussions on the topic.

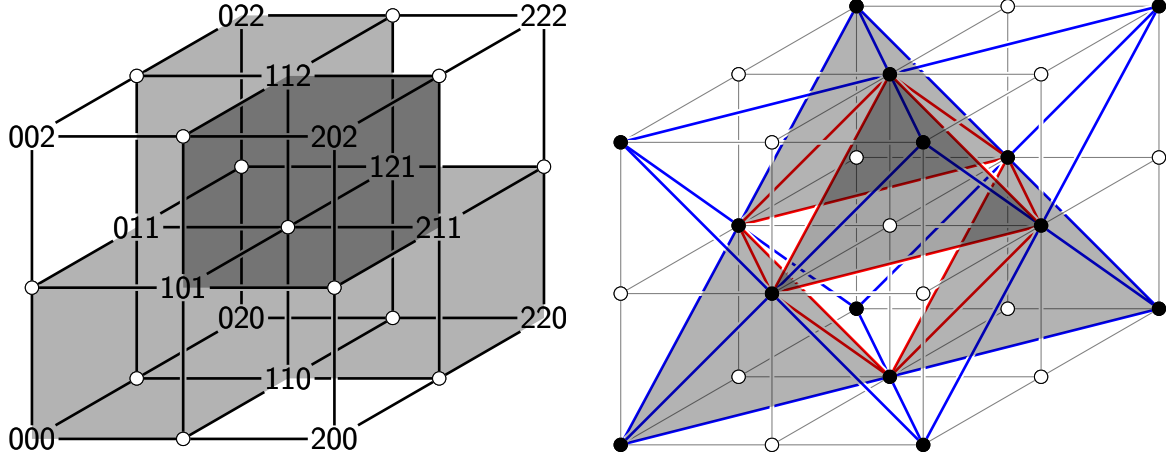


Figure 4. Left: A_3 identified with \mathbb{Z}_+^3 . Right: edges of A_3 , an octahedron is highlighted with red edges, black tetrahedra are shaded.

2 Combinatorics of A_3

We need the subsets of \mathbb{Z}^n

$$\mathbb{Z}_c^n = \{z \in \mathbb{Z}^n \mid \sum_{i=1}^n z_i = c\}, \quad (2.1)$$

$$\mathbb{Z}_+^n = \{z \in \mathbb{Z}^n \mid \sum_{i=1}^n z_i \in 2\mathbb{Z}\}, \quad (2.2)$$

$$\mathbb{Z}_-^n = \{z \in \mathbb{Z}^n \mid \sum_{i=1}^n z_i \in 2\mathbb{Z} + 1\}. \quad (2.3)$$

With this notation, the A_n lattice is defined as \mathbb{Z}_0^{n+1} . For A_3 we use the representation as the *octahedral lattice* \mathcal{L} , where $\mathcal{L} = \mathbb{Z}_+^3$. We will explain the bijection between A_3 and \mathcal{L} in Section 7, for now we do not need it.

For $n \in \mathbb{N}$ we denote the index set $[n] := \{1, 2, \dots, n\}$. For $i \in [n]$ let e_i be the i -th unit vector. In order to improve the readability of equations, we introduce the *shift operators* σ_i and $\sigma_{\bar{i}}$. For $i \in [n]$ and $z \in \mathbb{Z}^n$ the shift operators are defined by $\sigma_i z = z + e_i$ and $\sigma_{\bar{i}} z = z - e_i$. Additionally, if f is a function defined on a subset of \mathbb{Z}^n , the shift operator is defined by $\sigma_i f(z) = f(\sigma_i z)$. Moreover, if we give multiple numbers in the subscript this implies a composition of shift operators, for example $\sigma_{1,\bar{2}} = \sigma_1 \circ \sigma_{\bar{2}}$.

Let us explain the 3-cells of \mathcal{L} , see also Figure 4. The *octahedra* of \mathcal{L} are spanned by the points

$$\sigma_1 z, \sigma_{\bar{1}} z, \sigma_2 z, \sigma_{\bar{2}} z, \sigma_3 z, \sigma_{\bar{3}} z, \quad (2.4)$$

for all $z \in \mathbb{Z}_-^3$. We denote the set of octahedra by \mathcal{O} and identify $\mathcal{O} \simeq \mathbb{Z}_-^3$. The *tetrahedra* of \mathcal{L} come in two kinds. The *black tetrahedra* are spanned by the points

$$z, \sigma_{2,3} z, \sigma_{1,3} z, \sigma_{1,2} z, \quad (2.5)$$

for all $z \in \mathbb{Z}_+^3$, and the *white tetrahedra* are spanned by the points

$$\sigma_1 z, \sigma_2 z, \sigma_3 z, \sigma_{1,2,3} z, \quad (2.6)$$

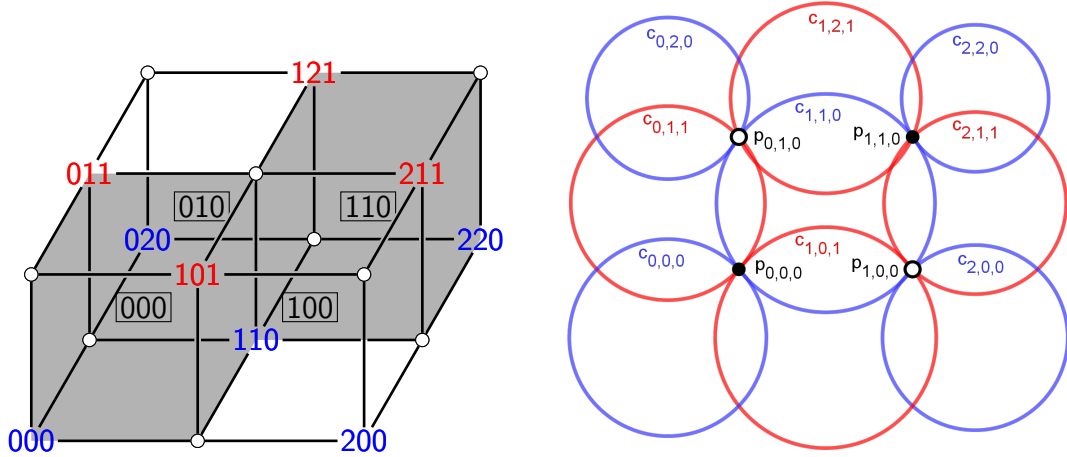


Figure 5. The 0-layer of a Miquel map (c, p) , defined on vertices and tetrahedra of \mathcal{L} (left), and its image in \mathbb{C} (right).

for all $z \in \mathbb{Z}_-^3$. We denote the set of tetrahedra by $\mathcal{T} \simeq \mathbb{Z}^3$, the set of black tetrahedra by $\mathcal{T}^\bullet \simeq \mathbb{Z}_+^3$, and the set of white tetrahedra by $\mathcal{T}^\circ \simeq \mathbb{Z}_-^3$. It is sometimes useful to think of the set of tetrahedra as corresponding to the cubes of \mathbb{Z}^3 .

Note that all the 2-cells of \mathcal{L} are triangles. We call two 3-cells adjacent if they share a triangle. We say a vertex $z \in \mathcal{L}$ is incident to a 3-cell if z is contained in the 3-cell.

3 Miquel maps

In this section we explain how we view the circles and intersection points of Miquel dynamics on the octahedral lattice \mathcal{L} .

Definition 3.1. A *Miquel map* (c, p) is a pair of maps

$$c : \mathcal{L} \rightarrow \text{Circles}(\hat{\mathbb{C}}), \quad (3.1)$$

$$p : \mathcal{T} \rightarrow \hat{\mathbb{C}}, \quad (3.2)$$

such that $p(T) \in c(z)$ for all incident $z \in \mathcal{L}$, $T \in \mathcal{T}$.

For $k \in \mathbb{Z}$, consider the restriction (c_k, p_k) of a Miquel map (c, p) to

$$\{z \in \mathcal{L} \mid z_3 \in \{k, k+1\}\} \cup \{T \in \mathcal{T} \mid T_3 = k\}, \quad (3.3)$$

in the sense that

$$c_k(i, j) = \begin{cases} c(i, j, k) & i + j + k \in 2\mathbb{Z}, \\ c(i, j, k+1) & i + j + k \in 2\mathbb{Z} + 1, \end{cases} \quad (3.4)$$

$$p_k(i, j) = p(i, j, k). \quad (3.5)$$

Thus, (c_k, p_k) is a circle pattern, see also Figure 5.

Consider an octahedron $O \in \mathcal{O}$. Then the six circles

$$\sigma_1 c(O), \sigma_{\bar{1}} c(O), \sigma_2 c(O), \sigma_{\bar{2}} c(O), \sigma_3 c(O), \sigma_{\bar{3}} c(O), \quad (3.6)$$

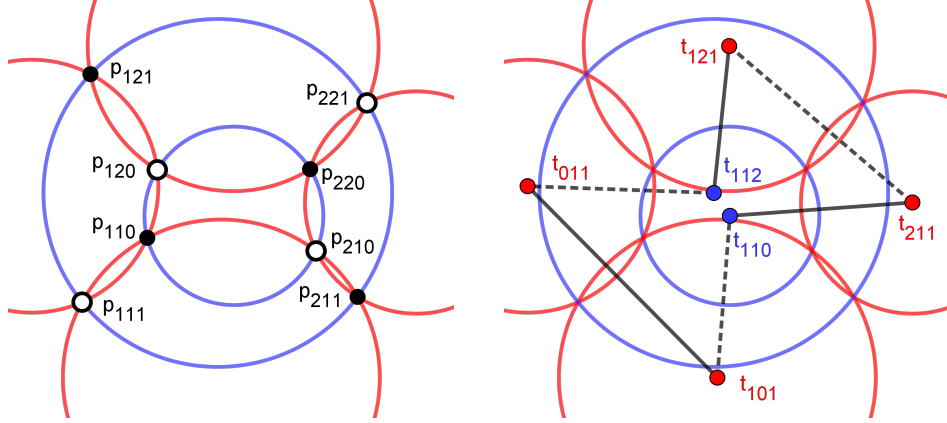


Figure 6. Coordinates in the octahedral lattice for a Miquel configuration at octahedron $(1, 1, 1)$.

of the vertices of O constitute a Miquel six circle configuration. The eight intersection points

$$\sigma_{\bar{1},\bar{2},\bar{3}}p(O), \sigma_{\bar{1},\bar{2}}p(O), \sigma_{\bar{1},\bar{3}}p(O), \sigma_{\bar{2},\bar{3}}p(O), \sigma_{\bar{1}}p(O), \sigma_{\bar{2}}p(O), \sigma_{\bar{3}}p(O), p(O), \quad (3.7)$$

of the eight tetrahedra adjacent to O are the intersection points of the Miquel configuration.

Each point $z \in \mathcal{L}$ with $z_3 = k + 2$ belongs to exactly one octahedron O with $O_3 = k + 1$, specifically $O = z - e_3$. Therefore each circle in (c_{k+1}, p_{k+1}) is determined via a Miquel configuration from (c_k, p_k) . Analogously, each tetrahedron $T \in \mathcal{T}$ with $T_3 = k + 1$ is adjacent to exactly one octahedron O with $O_3 = k + 1$. Therefore also all the intersection points of (c_{k+1}, p_{k+1}) are determined via Miquel configurations. We conclude that (c_{k+1}, p_{k+1}) is obtained from (c_k, p_k) via Miquel dynamics. Therefore Miquel maps are the lattice perspective on (the iteration of) Miquel dynamics.

4 dSKP maps

Definition 4.1. A *dSKP map* $a : \mathbb{Z}_{\pm} \rightarrow \hat{\mathbb{C}}$ is a map that satisfies the *dSKP lattice equation*, that is a map such that

$$\text{mr}(\sigma_1 a(z), \sigma_2 a(z), \sigma_3 a(z), \sigma_{\bar{1}} a(z), \sigma_{\bar{2}} a(z), \sigma_{\bar{3}} a(z)) = -1. \quad (4.1)$$

for all $z \in \mathbb{Z}_{\mp}$.

Before we turn to new results, let us quickly recapitulate a previously discovered result relating Miquel maps to dSKP maps. Given a Miquel map (c, p) we associate a *t-map* $t : \mathcal{L} \rightarrow \hat{\mathbb{C}}$, which consists of the circle centers of c , that is for $z \in \mathcal{L}$ the point $t(z)$ is the center of $c(z)$. The following theorem was found and proven in [Aff21] and independently in [KLRR22].

Theorem 4.2. The *t-map* of a Miquel map is a dSKP map.

Let us now turn to an analogous new result. For this, we need to split the intersection points of a Miquel map according to their parity on \mathbb{Z}^3 .

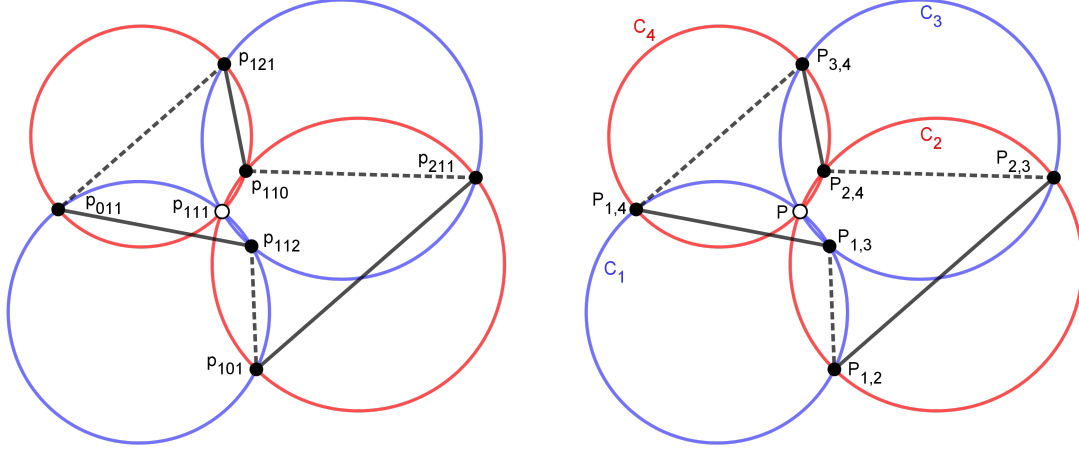


Figure 7. Left: coordinates in the octahedral lattice for a Clifford configuration at white tetrahedron $(1, 1, 1)$, the dSKP equation for p^\bullet is highlighted. Right: labeling for the proof of 4.4.

Definition 4.3. Let (c, p) be a Miquel map. The p^\bullet -map is the map $p^\bullet : \mathcal{T}^\bullet \rightarrow \hat{\mathbb{C}}$ -map which is the restriction of p to \mathcal{T}^\bullet . The p° -map is the map $p^\circ : \mathcal{T}^\circ \rightarrow \hat{\mathbb{C}}$ -map which is the restriction of p to \mathcal{T}° .

Theorem 4.4. The p^\bullet -map and p° -map of a Miquel map are dSKP maps.

Proof. It has been shown in [KS02] how the dSKP equation arises in a Clifford 4-circle configuration. Let us recall this result. Consider four circles C_1, C_2, C_3, C_4 that intersect in a point P , and let $P_{i,j}$ be the other intersection point of P_i and P_j for $i, j \in \{1, 2, 3, 4\}$, see also Figure 7. Then it was shown that

$$\text{mr}(P_{2,3}, P_{3,4}, P_{2,4}, P_{1,4}, P_{1,2}, P_{1,3}) = -1. \quad (4.2)$$

Now let us apply this result to our claim. Let $z \in \mathcal{L}$ and consider the identification of circles

$$c(z) = C_1, \quad \sigma_{1,3}c(z) = C_2, \quad \sigma_{1,2}c(z) = C_3, \quad \sigma_{2,3}c(z) = C_4. \quad (4.3)$$

All four circles pass through $p(z) = p^\circ(z)$, so we may identify $p^\circ(z) = P$. The remaining point identifications are

$$\sigma_2 p^\bullet(z) = P_{1,2}, \quad \sigma_1 p^\bullet(z) = P_{2,3}, \quad \sigma_2 p^\bullet(z) = P_{3,4}, \quad (4.4)$$

$$\sigma_1 p^\bullet(z) = P_{1,4}, \quad \sigma_3 p^\bullet(z) = P_{1,3}, \quad \sigma_3 p^\bullet(z) = P_{2,4}. \quad (4.5)$$

Therefore, the map p^\bullet satisfies

$$\text{mr}(\sigma_1 p^\bullet(z), \sigma_2 p^\bullet(z), \sigma_3 p^\bullet(z), \sigma_1 p^\bullet(z), \sigma_2 p^\bullet(z), \sigma_3 p^\bullet(z)) = -1, \quad (4.6)$$

as required by Definition 4.1. An analogous argument works for p° . \square

Remark 4.5. In [AdTM22] it was shown how values of the t -map t can be expressed in terms of initial data t^0, t^1 using dimer partition functions. The same tools apply to express the values of p^\bullet and p° in terms of initial data.

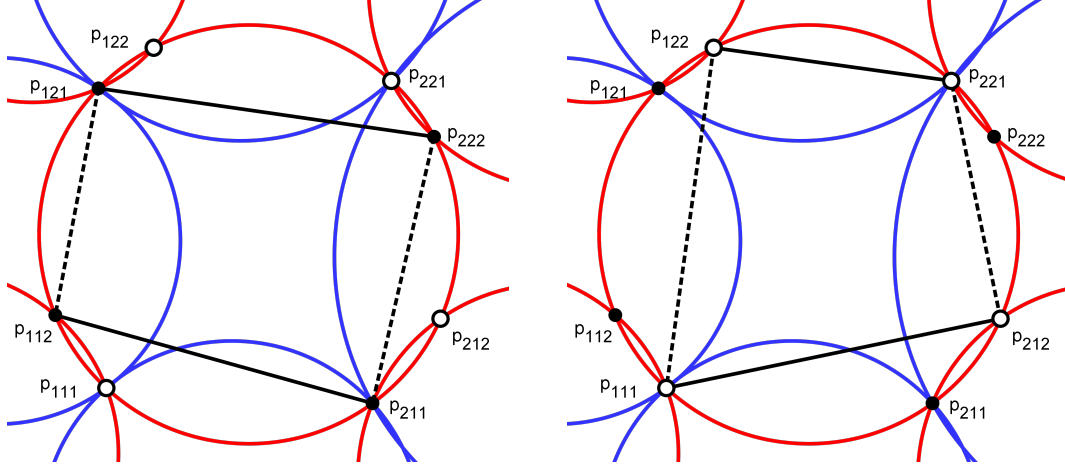


Figure 8. The points that define $X^\bullet(2, 2, 2)$ (left) and $X^\circ(2, 2, 2)$ (right) on the circle $C_{2,2,2}$.

5 Y-systems

Y-systems were introduced in [Zam91], see also further references in [ABS12] or [KNS11] for an overview. Y-systems are closely related to cluster algebras, as we will recall in Section 8.

Definition 5.1. We say a map $U : \mathbb{Z}_\pm \rightarrow \mathbb{C}$ is a *Y-system* if it satisfies

$$\sigma_3 U(z) \sigma_3 U(z) = \frac{(1 + \sigma_2 U(z))(1 + \sigma_{\bar{2}} U(z))}{(1 + \sigma_1 U^{-1}(z))(1 + \sigma_{\bar{1}} U^{-1}(z))}, \quad (5.1)$$

for all $z \in \mathbb{Z}_\mp$.

Let us recall the literature result relating Y-systems and Miquel maps.

Definition 5.2. Consider a Miquel map and let t be the associated t -map. The *Y-variables* $Y : \mathcal{O} \rightarrow \mathbb{R}$, are defined by

$$Y(z) := -\frac{(\sigma_{1,3} t(z) - t(z))(\sigma_{\bar{1},3} t(z) - t(z))}{(\sigma_{2,3} t(z) - t(z))(\sigma_{\bar{2},3} t(z) - t(z))}. \quad (5.2)$$

It was shown in [Aff21, KLRR22] that the Y -variables are real-valued. This is a condition on the relative angles of the four lines through $t(z)$ and through $\sigma_{1,3} t(z)$, $\sigma_{2,3} t(z)$, $\sigma_{\bar{1},3} t(z)$, $\sigma_{\bar{2},3} t(z)$ respectively. Since the intersection points $\sigma_{\bar{1},2} p(z)$, $\sigma_{\bar{2}} p(z)$, $p(z)$, $\sigma_{\bar{1}} p(z)$ are obtained from consecutively reflecting about the four lines, the composition of these four reflection is the identity. This imposes an angle condition on the four angles of consecutive lines, which in turn implies that $Y(z)$ is real-valued.

The first relation between Miquel maps and Y-systems was found in [Aff21] and independently in [KLRR22]. We recall this relation in the next theorem.

Theorem 5.3. The Y -variables of a Miquel map are a Y-system.

Now, let us present an analogous result for the p^\bullet - and p° -maps.

Definition 5.4. Consider a Miquel map and the associated p^\bullet , p° maps. The X^\bullet -variables $X^\bullet : \mathcal{L} \rightarrow \mathbb{R}$, are defined by

$$X^\bullet(z) := -\text{cr}(\sigma_{\bar{1},2} p^\bullet(z), \sigma_{\bar{2},3} p^\bullet(z), p^\bullet(z), \sigma_{\bar{1},3} p^\bullet(z)). \quad (5.3)$$

Analogously, the X° -variables $X^\circ : \mathcal{L} \rightarrow \mathbb{R}$, are defined by

$$X^\circ(z) := -\text{cr}(\sigma_{\bar{1},\bar{2},\bar{3}}p^\circ(z), \sigma_{\bar{2}}p^\circ(z), \sigma_{\bar{3}}p^\circ(z), \sigma_{\bar{1}}p^\circ(z)). \quad (5.4)$$

As mentioned in the introduction, the X^\bullet - and X° -variables are real-valued, since they are cross-ratios of four points on a circle, see also Figure 8.

Theorem 5.5. The X^\bullet -variables and the X° -variables of a Miquel map are a Y-system.

Proof. In Theorem 4.4 we have shown that p^\bullet -maps are dSKP maps. The X^\bullet -variables that we defined in Definition 5.4 for p^\bullet -maps have been previously introduced for general dSKP maps in [ABS12, Section 7] as h -variables, with opposite sign. \square

Since the X -variables constitute a Y-system, we see that positivity of the X -variables is also preserved under Miquel dynamics. Of course, whether an X -variable is positive or not depends on the order in which the four points of p^\bullet (resp. p°) appear on the corresponding circle. However, it is not directly clear in what manner this characterizes the corresponding circle pattern.

Question 5.6. Is there a geometric characterization of circle patterns that have positive X^\bullet - and or X° -variables? Is there a reasonable notion of p^\bullet -embedding (resp. p° -embedding) that has positive X^\bullet -variables (X° -variables)? Does every t -embedding belong to a circle pattern with positive X^\bullet - and or X° -variables?

Since X^\bullet and X° satisfy the same lattice equation (as a Y-system), it is possible that $X^\bullet(z) = X^\circ(z)$ for all $z \in \mathcal{L}$. A practical technique to construct “regular looking” larger patches of a circle pattern is to just take a rectangular lattice for the intersection points of the circle pattern. Experiments show that Miquel maps that contain such a rectangular circle pattern do indeed satisfy $X^\bullet = X^\circ$, which leads us to ask a question.

Question 5.7. Is there a geometric characterization of all circle patterns or Miquel maps that satisfy $X^\bullet = X^\circ$?

This question may relate to our results on h -embeddings, see Section 9, we did not investigate this direction further.

Next, we explain how the Y - and X -variables determine a Miquel map up to boundary data. The k -th layer of a Y-system $U : \mathbb{Z}_\pm^3 \rightarrow \mathbb{C}$ is the restriction of U to $\{z \in \mathbb{Z}_\pm^3 \mid z_3 \in \{k, k+1\}\}$.

Let us begin with the Y -variables. Let t_k be the restriction of a t -map t to all $z \in \mathcal{L}$ such that $z_3 = k$. Then t_k determines all of t , since Theorem 4.2 determines t_{k+1} and t_{k-1} given t_k . The conical net t does not determine t . Instead, we may choose one of the intersection points freely and only then does the t -map determine all of the Miquel map.

Theorem 5.8. Let (c, p) be a Miquel map, and let t_k be the conical net of (c_k, p_k) . The t -map is uniquely determined by the 0-th layer of the Y -variables and the boundary data

$$\{t(z) \mid z \in \mathcal{L}, z_2 = 0, 1, z_3 = 0, 1\}. \quad (5.5)$$

Generically, any real-valued Y-system is the Y -variables of a t -map.

Proof. Let us explain how the 0-th layer of the Y -variables determines t_0 up to boundary data. Assume we know $Y(z)$ with $z_3 = 0$ and t on $\sigma_{1,3}z, \sigma_{\bar{1},3}z, \sigma_{2,3}z$. Then we may solve Equation (5.2) uniquely for $\sigma_{2,3}z$. For $z_3 = 1$, a quick calculation shows that

$$Y(z) = -\frac{(t(\sigma_{2,3}z) - t(z))(t(\sigma_{\bar{2},3}z) - t(z))}{(t(\sigma_{1,3}z) - t(z))(t(\sigma_{\bar{1},3}z) - t(z))}. \quad (5.6)$$

Therefore, if we know $Y(z)$ with $z_3 = 1$ the point $\sigma_{2,3}z$ is determined by $\sigma_{1,3}z, \sigma_{\bar{1},3}z, \sigma_{\bar{2},3}z$. Now, if we choose boundary data as in the claim, all of t_0 is determined by the 0-th layer of the Y -variables. Since the Y -variables are real, t_0 is indeed a conical net. The whole t -map is then determined by Miquel dynamics. \square

Now let us prepare the analogous result for the X^\bullet -variables (and analogously the X° -variables). Assume we know p^\bullet but not p° . For every $z \in \mathcal{L}$, the circle $c(z)$ contains four points of p^\bullet , therefore all the circles are determined by p^\bullet . As a consequence, also all the intersection points p are determined. Thus, p^\bullet (or p°) determine the Miquel map uniquely.

Recall that $p_k(z)$ is the restriction of p to all $z \in \mathcal{L}$ with $z_3 = k$. We define the restriction p_k^\bullet slightly differently, as the restriction of p^\bullet to $z \in \mathcal{L}$ with $z_3 \in \{k, k+1\}$. With this definition, the restriction p_k^\bullet determines all of p^\bullet , since we may use Theorem 4.4 to determine p_{k+1}^\bullet and p_{k-1}^\bullet from p_k^\bullet .

Theorem 5.9. Let (c, p) be a Miquel map. Then (c, p) is uniquely determined by the 0-th layer of the X^\bullet -variables and the boundary data

$$\{p^\bullet(z) \mid z \in \mathbb{Z}, z_1 + z_2 \in \{0, 1\}, z_1 - z_2 \in \{0, 1\}, z_3 \in \{0, 1\}\}. \quad (5.7)$$

Generically, any real-valued Y -system is the X^\bullet -variables of some Miquel map. The analogous two statements hold for p° -maps and X° -variables.

Proof. Let us explain how the 0-th layer of the X^\bullet -variables determines p_0^\bullet up to boundary data. The boundary data in the claim corresponds to a two pairs of consecutive diagonals of p_0^\bullet . Assume we know $X^\bullet(z)$ with $z_3 = 1$ and p^\bullet on $\sigma_{\bar{1},\bar{2},3}z, \sigma_{\bar{1}}z, \sigma_{\bar{2}}z, \sigma_{\bar{3}}z$. Then may solve Equation (5.3) for $\sigma_{2,3}z$. However, we need a second multi-ratio equation to propagate to all of \bullet_0 . Let $z \in \mathcal{L}$ and consider the three quantities

$$\text{cr}(\sigma_3 p^\bullet(z), \sigma_1 p^\bullet(z), \sigma_{1,2,3} p^\bullet(z), \sigma_2 p^\bullet(z)), \quad (5.8)$$

$$\text{mr}(\sigma_{\bar{1}} p^\bullet(z), \sigma_{\bar{3}} p^\bullet(z), \sigma_{\bar{2}} p^\bullet(z), \sigma_1 p^\bullet(z), \sigma_3 p^\bullet(z), \sigma_2 p^\bullet(z)), \quad (5.9)$$

$$\sigma_{1,2} \text{mr}(\sigma_3 p^\bullet(z), \sigma_{\bar{2}} p^\bullet(z), \sigma_1 p^\bullet(z), \sigma_{\bar{3}} p^\bullet(z), \sigma_2 p^\bullet(z), \sigma_{\bar{1}} p^\bullet(z)). \quad (5.10)$$

The cross-ratio is equal to $\sigma_{1,2,3}X(z)$ (Definition 5.4), the multi-ratios are both equal to -1 , since they are instances of the dSKP equation (Theorem 4.4). Therefore the product of the three quantities is equal to $\sigma_{1,2,3}X(z)$, but also due to edge-cancellations to

$$\text{mr}(\sigma_{\bar{1}} p^\bullet(z), \sigma_{\bar{3}} p^\bullet(z), \sigma_{\bar{2}} p^\bullet(z), \sigma_1 p^\bullet(z), \sigma_{1,1,2} p^\bullet(z), \sigma_{1,2,\bar{3}} p^\bullet(z), \sigma_{1,2,2} p^\bullet(z), \sigma_2 p^\bullet(z)). \quad (5.11)$$

Therefore, we know the values of these multi-ratios, which is $\sigma_{1,2,3}X(z)$. Note that these multi-ratios involve only points of p_0^\bullet , which means we can solve any one of them for one of the points involved, assuming we know the other seven points. It is now straightforward to verify that we may propagate the initial data to all of p_0^\bullet . As explained before, p_0^\bullet determines all of p^\bullet , which in turn determines (c, p) uniquely. Note that the fact that the X^\bullet -variables are real ensures that the appropriate points of p^\bullet are on circles. \square

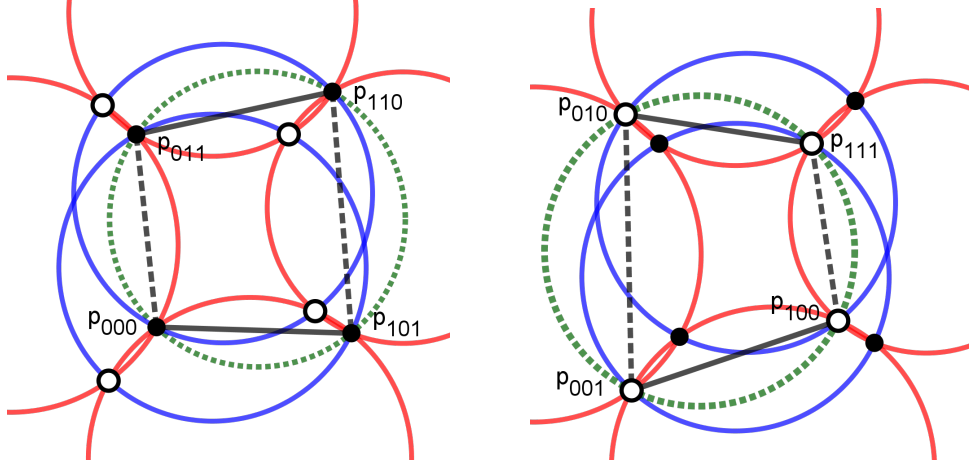


Figure 9. The points that define $W^\bullet(1, 1, 1)$ (left) and $W^\circ(1, 1, 1)$ (right) in the Miquel configuration at the octahedron $(1, 1, 1)$. This is a special case of a Miquel configuration in an integrable circle pattern, in which two additional (green, dotted) circles exist.

6 Integrable circle patterns

In Section 4 we showed that the p^\bullet -map defined on \mathcal{T}^\bullet is a dSKP map. Then we introduced the X^\bullet -variables in Section 5 and showed that the X^\bullet -variables are a Y-system. As we explained, the X^\bullet -variables coincide with the general Y-system associated to a dSKP map in [ABS12]. Note that if we identify the black tetrahedra \mathcal{T}^\bullet with a copy of \mathcal{L} , let us say \mathcal{L}' , then the X -variables are cross-ratios of one type of tetrahedra of \mathcal{L}' . However, there are two types of tetrahedra in \mathcal{L}' . Therefore, we may also consider cross-ratios of the other type of tetrahedra.

Definition 6.1. Consider a Miquel map and the associated p^\bullet, p° maps. The W^\bullet -variables $W^\bullet : \mathcal{O} \rightarrow \mathbb{C}$, are defined by

$$W^\bullet(z) := -\text{cr}(\sigma_{\bar{1},\bar{2},\bar{3}}p^\bullet(z), \sigma_{\bar{2}}p^\bullet(z), \sigma_{\bar{3}}p^\bullet(z), \sigma_{\bar{1}}p^\bullet(z)). \quad (6.1)$$

Analogously, the W° -variables $X^\circ : \mathcal{O} \rightarrow \mathbb{C}$, are defined by

$$W^\circ(z) := -\text{cr}(\sigma_{\bar{1},\bar{2}}p^\circ(z), \sigma_{\bar{2},\bar{3}}p^\circ(z), p^\circ(z), \sigma_{\bar{1},\bar{3}}p^\circ(z)). \quad (6.2)$$

Note that the W -variables are generally complex-valued, not real-valued. However, they satisfy the same recursion law as the X -variables.

Theorem 6.2. The W^\bullet -variables and the W° -variables of a Miquel map are a Y-system.

Proof. Same as proof of Theorem 4.4. □

The W^\bullet - and W° -variables are actually directly related.

Theorem 6.3. The W^\bullet - and W° -variables are complex conjugates, that is for all $z \in \mathcal{O}$ holds $W^\circ(z) = \overline{W^\bullet(z)}$.

Proof. To simplify notation, define

$$P = \sigma_{\bar{1},\bar{2},\bar{3}}p^\bullet(z), \quad P_{3,1} = \sigma_{\bar{2}}p^\bullet(z), \quad P_{1,2} = \sigma_{\bar{3}}p^\bullet(z), \quad P_{2,3} = \sigma_{\bar{1}}p^\bullet(z), \quad (6.3)$$

$$P_3 = \sigma_{\bar{1},\bar{2}}p^\circ(z), \quad P_1 = \sigma_{\bar{2},\bar{3}}p^\circ(z), \quad P_{1,2,3} = p^\circ(z), \quad P_2 = \sigma_{\bar{1},\bar{3}}p^\circ(z). \quad (6.4)$$

We normalize $P = 0$, $P_{1,2,3} = \infty$. Let $i \in [3]$ and consider the crossratios

$$\lambda_{i,i+1} = \text{cr}(P_i, P, P_{i+1}, P_{i,i+1}) \in \mathbb{R}. \quad (6.5)$$

Solving this equation for $P_{i,i+1}$ gives

$$P_{i,i+1} = \frac{\lambda_{i,i+1} - 1}{\lambda_{i,i+1}P_i^{-1} - P_{i+1}^{-1}}. \quad (6.6)$$

However, the three cross-ratios $\lambda_{1,2}, \lambda_{2,3}, \lambda_{3,1}$ are not independent, since for each $i \in [3]$ the three points $P_i, P_{i-1,i}, P_{i,i+1}$ need to be on a line. The colinearity condition is equivalent to

$$\frac{P_{i-1,i} - P_i}{P_{i,i+1} - P_i} \in \mathbb{R}. \quad (6.7)$$

Inserting Expressions (6.6) yields

$$\frac{(\bar{P}_i - \bar{P}_{i+1})(P_{i-1} - P_i)}{(P_i - P_{i+1})(\bar{P}_{i-1} - \bar{P}_i)} = \frac{(\bar{P}_i - \lambda_{i,i+1}\bar{P}_{i+1})(P_{i-1} - \lambda_{i-1,i}P_i)}{(P_i - \lambda_{i,i+1}P_{i+1})(\bar{P}_{i-1} - \lambda_{i-1,i}\bar{P}_i)}. \quad (6.8)$$

The product of the three instances of this equation yields the trivial equation $1 = 1$, which is a proof of Miquel's theorem. The claim in the theorem is equivalent to

$$\text{cr}(P_{1,2,3}, P_1, P_2, P_3) = \overline{\text{cr}(P, P_{2,3}, P_{3,1}, P_{1,2})}. \quad (6.9)$$

We may solve Equation (6.8) for $\lambda_{2,3}$ and $\lambda_{3,1}$ and insert these into Equation (6.9), and also insert the expressions (6.6). In this way we obtain a rational equation in the formal variables

$$P_1, P_2, P_3, \bar{P}_1, \bar{P}_2, \bar{P}_3, \lambda_{1,2} \quad (6.10)$$

A computer algebra software will then confirm that Equation (6.9) holds. \square

Remark 6.4. Although Theorem 6.3 appears to be rather elementary, we did not find a simpler proof. We were also not able to find the theorem in the literature, although we are not sure that it is new. Note that in terms of Möbius geometry, the theorem states that there is an orientation-reversing Möbius transformation that maps $P, P_{1,2}, P_{2,3}, P_{3,1}$ to $P_{1,2,3}, P_3, P_1, P_2$.

Due to Theorem 6.2, if the initial W^\bullet -variables are real, then all W^\bullet -variables are real. Moreover, due to Theorem 6.3, if the W^\bullet -variables are real, so are the W° -variables. Therefore, let us briefly discuss the case of real W -variables.

Consider an edge $e = (v, v') = (f, f')^* \in E(\mathbb{Z}^2)$ with v, f, v', v' in counterclockwise order, as well as a circle pattern (c, p) with conical net t . We call the *edge cross-ratio* $\gamma(e)$ the cross-ratio

$$\gamma(e) = \text{cr}(t(v), p(f), t(v'), p(f')). \quad (6.11)$$

Note that the edge cross-ratio has absolute value 1, and the argument is the intersection angle of $c(v)$ and $c(v')$.

Definition 6.5. An *integrable circle pattern* [BMS05] is a circle pattern such that for each vertex $v \in V$ holds

$$\gamma(e_1)\gamma(e_2)\gamma(e_3)\gamma(e_4) = 1, \quad (6.12)$$

where e_1, e_2, e_3, e_4 are the four edges containing v .

Theorem 6.6. Let (c, p) be a Miquel map. The following are equivalent:

- (i) W^\bullet, W° are real-valued,
- (ii) $W^\bullet = W^\circ$,
- (iii) (c_k, p_k) is an integrable circle pattern for all $k \in \mathbb{Z}$.

Proof. The equivalence of (i) and (ii) is clear due to Theorem 6.3. Next, we explain the equivalence of (i) and (iii). In [Aff21], it was proven that a Miquel configuration is part of an integrable circle pattern if and only if the four intersection points $\sigma_{\bar{1},\bar{2},\bar{3}}p^\bullet(z), \sigma_{\bar{2}}p^\bullet(z), \sigma_{\bar{3}}p^\bullet(z), \sigma_{\bar{1}}p^\bullet(z)$ are on a circle, or equivalently the four intersection points $\sigma_{\bar{1},\bar{2}}p^\circ(z), \sigma_{\bar{2},\bar{3}}p^\circ(z), p^\circ(z), \sigma_{\bar{1},\bar{3}}p^\circ(z)$ are on a circle. The W^\bullet -variables are minus the cross-ratio of the first four points, which is real if and only if these points are on a circle, which proves the claim. \square

Note that in [KLRR22] the fixed points of Miquel dynamics were also considered. In particular, they showed that orthogonal circle patterns and certain circle patterns with constant intersection angles are fixed points of Miquel dynamics. It is not hard to see that these are special cases of integrable circle patterns. Another special case of integrable circle patterns are *isoradial graphs*, see [BdT12].

Remark 6.7. There is an equivalent definition of integrable circle patterns, requiring that the edge cross-ratios γ factorize onto zig-zag paths of \mathbb{Z}^2 . More specifically, a zig-zag is a path that turns maximally right and then maximally left in alternating fashion. To each zig-zag we associate a complex number in $\mathbb{S}^1 \subset \mathbb{C}$. In an integrable circle pattern, each cross-ratio $\gamma(e)$ is the ratio of the two complex numbers associated to the zig-zags. The effect of Miquel dynamics on an integrable circle pattern is to interchange the complex numbers associated to zig-zags in every second adjacent pair.

Remark 6.8. One can also consider circle patterns (c, p) on \mathbb{Z}^3 , for which we switch the role of faces and vertices. That is we consider maps

$$p : \mathbb{Z}^3 \rightarrow \hat{\mathbb{C}}, \quad c : F(\mathbb{Z}^3) \rightarrow \text{Circles}(\hat{\mathbb{C}}), \quad (6.13)$$

such that $p(v) \in c(f)$ whenever $v \in f$. By using Miquel's theorem it is possible to show that these circle patterns exist and are uniquely defined from 2-dimensional boundary data given on the coordinate planes of \mathbb{Z}^3 . Theorem 6.3 tells us that propagation from boundary data is governed by

$$\text{cr}(p(z), \sigma_{1,3}p(z), \sigma_{1,2}p(z), \sigma_{2,3}p(z)) = \overline{\text{cr}(p(\sigma_{1,2,3}z), \sigma_2p(z), \sigma_3p(z), \sigma_1p(z))}. \quad (6.14)$$

The same equation without the complex conjugation on the right-hand-side is known as the *double cross-ratio equation* [NS97]. As a consequence, if we take a circle pattern on \mathbb{Z}^3 and apply complex conjugation to every second point, the result will be a solution of the double cross-ratio equation.

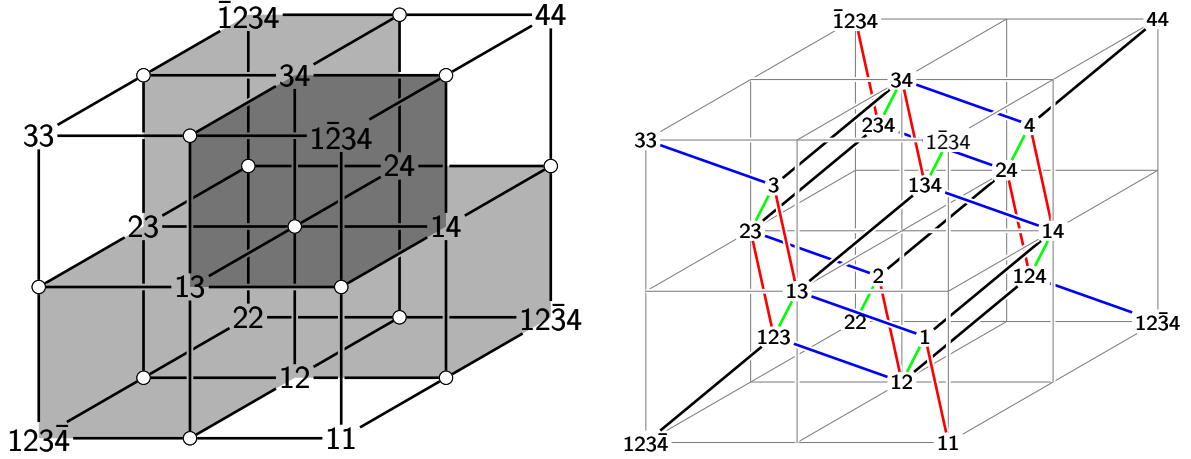


Figure 10. Left: identification of \mathcal{L} with A_3 . Right: identification of $\mathcal{L} \cup \mathcal{T}^\bullet \cup \mathcal{T}^\circ$ with $\hat{A}_4 \subset A_4$ (red, green, blue, black correspond to the 1-, 2-, 3-, 4-direction respectively). To improve the readability of the figure, we use shift notation, every label I corresponds to $\sigma_I(z)$ for a point $z \in \mathbb{Z}_{-2}^5$, and we suppressed the 5th coordinate.

7 A combined dSKP map on A_4

We need some combinatorial and geometric preliminaries. We begin with combinatorics. Let us recall the definition of the A_4 lattice, namely

$$A_4 = \mathbb{Z}_0^5 = \{z \in \mathbb{Z}^5 \mid \sum_{i=1}^5 z_i = 0\}. \quad (7.1)$$

In the following, we consider the subset

$$\hat{A}_4 = \{z \in A_4 \mid z_5 \in \{-1, 0, 1\}\}. \quad (7.2)$$

Next, we introduce an identification $\phi : \hat{\mathcal{L}} \rightarrow \hat{A}_4$ of $\hat{\mathcal{L}} := \mathcal{L} \cup \mathcal{T}$ with \hat{A}_4 as follows, see also Figure 10. Let us identify \mathcal{T} with the cubes of \mathbb{Z}^3 , which in turn we identify with $\mathbb{Z}^3 + \frac{1}{2}(1, 1, 1)$. Introduce the four vectors in \mathbb{Z}^5

$$a_1 = (1, 0, 0, 0, -1), \quad a_2 = (0, 1, 0, 0, -1), \quad (7.3)$$

$$a_3 = (0, 0, 1, 0, -1), \quad a_4 = (0, 0, 0, 1, -1), \quad (7.4)$$

and the four vectors in $\frac{1}{2}\mathbb{Z}^3$

$$b_1 = \frac{1}{2}(+1, -1, -1), \quad b_2 = \frac{1}{2}(-1, +1, -1), \quad (7.5)$$

$$b_3 = \frac{1}{2}(-1, -1, +1), \quad b_4 = \frac{1}{2}(+1, +1, +1). \quad (7.6)$$

Set $\phi(0) = 0$. Let $z \in \mathcal{L} = \mathbb{Z}_+^3$ and $z' \in \mathcal{T} = \mathbb{Z}^3 + \frac{1}{2}(1, 1, 1)$ such that z is a vertex of the tetrahedron z' , then we require that for every $i \in [4]$ holds

$$\phi(z) - \phi(z') = \begin{cases} +a_i & \text{if } z - z' = +b_i, \\ -a_i & \text{if } z - z' = -b_i. \end{cases} \quad (7.7)$$

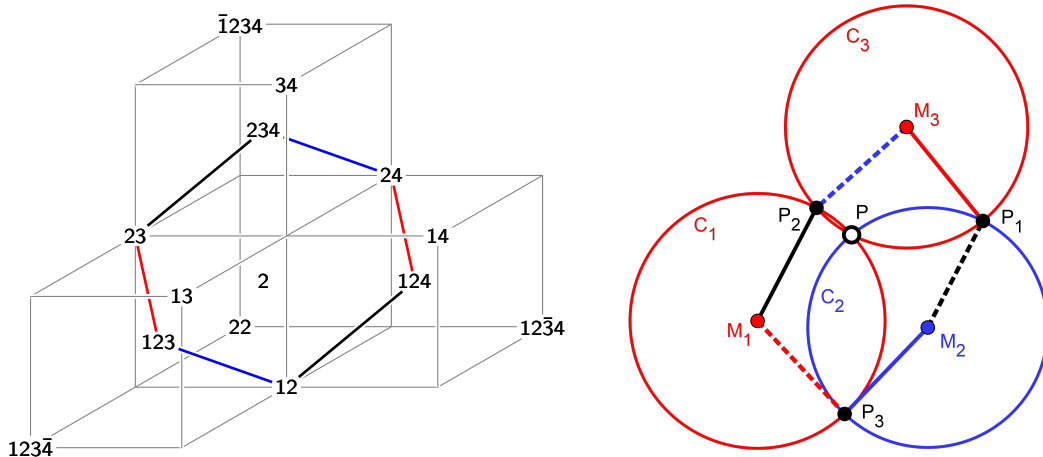


Figure 11. Left: an octahedron in \hat{A}_4 , with three vertices corresponding to \mathcal{L} and three to \mathcal{T}^\bullet . Right: the corresponding geometric configuration with labels as in Lemma 7.2.

This defines ϕ on all of $\hat{\mathcal{L}}$. Since we gave a definition of ϕ via differences, we have to check that this is well-defined. Each closing conditions corresponds to a (planar) rhombus in $\mathcal{L} \cup \mathcal{T}$, involving two vertices of \mathcal{L} , a tetrahedron of \mathcal{T}^\bullet and a tetrahedron of \mathcal{T}° . Opposite edges in the rhombus are mapped to the same difference by ϕ , therefore ϕ is well-defined.

Since all the a_i vectors are in A_5 , so is all of $\phi(\hat{\mathcal{L}})$. The restriction of ϕ to \mathcal{L} has constant coordinate $z_5 = 0$, the restriction to \mathcal{T}^\bullet has constant coordinate $z_5 = 1$ and the restriction to \mathcal{T}° has constant coordinate $z_5 = -1$. This reflects the fact that $\mathcal{L} \simeq A_3$, $\mathcal{T}^\bullet \simeq A_3$ and $\mathcal{T}^\circ \simeq A_3$.

Using the identification of $\hat{\mathcal{L}}$ with \hat{A}_4 via ϕ , we may consider a combined map $(p^\bullet, t, p^\circ) : \hat{\mathcal{L}} \rightarrow \mathbb{C}$. Fix $m \in [5]$, set

$$I = [5] \setminus \{m\}, \quad (7.8)$$

and let $z \in \mathbb{Z}_{-2}^5$. Then the six points

$$\{\sigma_{i_1, i_2} z \mid i_1, i_2 \in I, i_1 \neq i_2\}, \quad (7.9)$$

are the vertices of an octahedron in A_4 , and every octahedron may be represented in this way. If $m = 5$, we recover the octahedra that live in only one of the lattices \mathcal{L} , \mathcal{T}^\bullet or \mathcal{T}° . For $m \neq 5$, the octahedra involve three vertices of \mathcal{L} and three vertices of either \mathcal{T}^\bullet or \mathcal{T}° .

Definition 7.1. A *dSKP map* $a : A_n \rightarrow \hat{\mathbb{C}}$ is a map that satisfies the *dSKP lattice equation*, that is a map such that

$$\text{mr}(a(\sigma_{i_1, i_2} z), a(\sigma_{i_2, i_3} z), a(\sigma_{i_1, i_3} z), a(\sigma_{i_3, i_4} z), a(\sigma_{i_1, i_4} z), a(\sigma_{i_2, i_4} z)) = -1, \quad (7.10)$$

for all $\{i_1, i_2, i_3, i_4\} \in \binom{[n]}{4}$, and $z \in \mathbb{Z}_{-2}^{n+1}$.

To show how the t -, p^\bullet - and p° -maps are a dSKP map on A_4 , we also need a geometric lemma. From the viewpoint of hyperbolic geometry, this lemma is actually about two related ideal tetrahedra, but we give an elementary proof.

Lemma 7.2. Consider three circles C_1, C_2, C_3 that intersect in a point P , and let P_1, P_2, P_3 be the other three intersection points, see Figure 11. Let M_1, M_2, M_3 be the corresponding circle centers. Then we have

$$\text{mr}(P_1, M_3, P_2, M_1, P_3, M_2) = -1. \quad (7.11)$$

Proof. Since multi-ratios are invariant under Möbius transformations, we may normalize the configuration with a Möbius transformation M such that $M(P) = \infty$ and $M(\infty) = 0$. As a consequence, we may assume C_1, C_2, C_3 are straight lines and M_1, M_2, M_3 are the reflections of 0 about the lines P_2P_3, P_1P_3, P_1P_2 . In complex numbers, this implies that

$$M_3 = P_1 - \bar{P}_1 \frac{P_2 - P_1}{\bar{P}_2 - \bar{P}_1}, \quad (7.12)$$

and analogous formulas for M_1 and M_2 . Moreover, we calculate that

$$M_3 - P_1 = -\bar{P}_1 \frac{P_2 - P_1}{\bar{P}_2 - \bar{P}_1}, \quad M_3 - P_2 = -\bar{P}_2 \frac{P_1 - P_2}{\bar{P}_1 - \bar{P}_2}. \quad (7.13)$$

In turn, this implies

$$\frac{M_3 - P_1}{M_3 - P_2} = \frac{\bar{P}_1}{\bar{P}_2}. \quad (7.14)$$

Inserting this and the two other analogous ratios into the multi-ratio in the claim yields the desired result. \square

Remark 7.3. Note that by combining several copies of the equation of Lemma 7.2 in one cube of a Miquel six circle configuration, one may obtain alternative proofs for both Theorem 4.2 and Theorem 5.8.

Theorem 7.4. Given a Miquel map, the associated dSKP maps p^\bullet, t, p° are a dSKP map on \hat{A}_4 , via the identification ϕ of \hat{A}_4 with $\hat{\mathcal{L}}$.

Proof. For octahedra that do not involve direction 5, the dSKP equation follows from Theorem 4.2 and Theorem 4.4. Each other octahedron involves three circles intersecting in a common point. More specifically, consider $z \in \mathbb{Z}_{-2}^5$ and let $J \in \binom{[5]}{4}$ be such that $J \cup \{5\} = \{i_1, i_2, i_3, 5\}$. Then the three vertices $\sigma_{i,5}z$ for $i \in J$ and the three vertices $\sigma_{i,j}z$ for $i, j \in J, i \neq j$ make up such an octahedron. In Figure 11, we illustrate an example of such an octahedron and how this octahedron is situated in $\mathcal{L} \cup \mathcal{T}^\bullet$. Therefore, the dSKP equation involves three circle centers of t and three intersection points of either p^\bullet or p° as required for Lemma 7.2 to apply, which concludes the proof. \square

Remark 7.5. In a sense, Theorem 7.4 states that p^\bullet (and p°) is a *Bäcklund transform* of t in A_4 , since these are defined on adjacent copies of A_3 , similar to how Bäcklund transforms are usually two solutions on adjacent copies of \mathbb{Z}^2 in \mathbb{Z}^3 . Moreover, using Lemma 7.2 one can show that t together with 1-dimensional initial data of p^\bullet , determines all of p^\bullet , and vice versa. The same holds with p° .

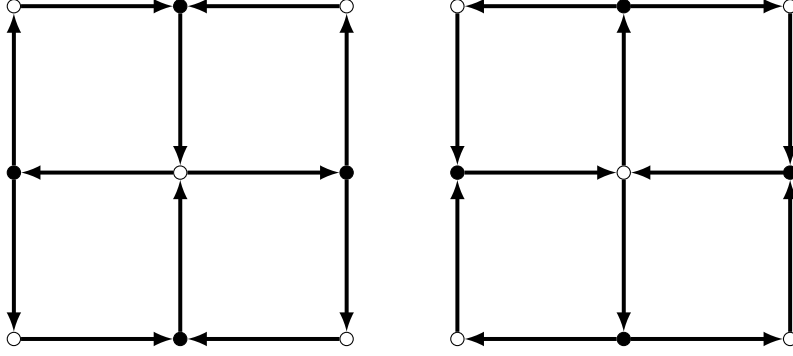


Figure 12. The square grid quivers S_0 (left) and S_1 (right). Mutating in S_0 at all the black vertices (or all the white vertices) yields S_1 and vice versa.

8 Cluster algebras

Let us briefly explain how our results relate to cluster algebras [FZ01, GR17]. Both relations are well established but may not be familiar to the reader with a background in discrete integrable systems or geometry.

A *quiver* is a graph $G = (V, E)$ together with an anti-symmetric form $\nu : V \times V \rightarrow \mathbb{Z}$. Graphically, we may represent ν as a drawing as follows: for each edge $(v, v') \in E$ draw $|\nu_{v,v'}|$ arrows from v to v' if $\nu_{v,v'}$ is positive and from v' to v otherwise. We only consider two kinds of quivers in the following. For $k \in \{0, 1\}$ we define the *square grid quiver* S_k on the vertex set \mathbb{Z}^2 by

$$\nu_{(i,j),(i+1,j)} = (-1)^{i+j+k}, \quad \nu_{(i,j),(i,j+1)} = (-1)^{i+j+k+1}, \quad (8.1)$$

and $\nu_{v,v'} = 0$ if $|v - v'| > 1$. For $k \in 2\mathbb{Z}$ we set $S_k = S_0$ and for $k \in 2\mathbb{Z} + 1$ we set $S_k = S_1$.

A *mutation at vertex* $v \in Q$ of a quiver Q produces a new quiver \tilde{Q} . We only need the case that for all $v, v' \in V$ holds $\nu_{v,v'} \in \{-1, 0, 1\}$. In this case, the new quiver \tilde{Q} is determined by

$$\tilde{\nu}_{v_1 v_2} = \begin{cases} -\nu_{v_1 v_2} & \text{if } v \in \{v_1, v_2\}, \\ \nu_{v_1 v_2} + \Theta(\nu_{v_1 v})\Theta(\nu_{v v_2}) - \Theta(\nu_{v_2 v})\Theta(\nu_{v v_1}) & \text{otherwise,} \end{cases} \quad (8.2)$$

where $\Theta(x) = \max(0, x)$. Consider the square grid quiver S_k . Mutating at every vertex $(i, j) \in \mathbb{Z}^2$ such that $i + j + k \in 2\mathbb{Z}$ produces S_{k+1} (simultaneously or in arbitrary order).

Consider a function $\mathcal{X} : V \rightarrow \mathbb{C}$ on the vertices of the quiver, which we call *cluster variables*. Assume again that for all $v, v' \in V$ holds $\nu_{v,v'} \in \{-1, 0, 1\}$. Then, for mutation at a vertex $v \in V$, the new cluster variables $\tilde{\mathcal{X}}$ after mutation are related to the old cluster variables \mathcal{X} before mutation by

$$\tilde{\mathcal{X}}(v') = \begin{cases} \mathcal{X}(v)^{-1} & \text{if } v' = v, \\ \mathcal{X}(v')(1 + \mathcal{X}(v)) & \text{if } (v, v') \text{ is an arrow,} \\ \mathcal{X}(v')(1 + \mathcal{X}(v)^{-1})^{-1} & \text{if } (v', v) \text{ is an arrow,} \\ \mathcal{X}(v') & \text{otherwise.} \end{cases} \quad (8.3)$$

Consider the square grid quiver S_0 with cluster variables $\mathcal{X}_0 : \mathbb{Z}^2 \rightarrow \mathbb{C}$ and the sequence

of mutations that takes S_0 to S_1 . In this case the new cluster variables \mathcal{X}_1 are

$$\mathcal{X}_1(i, j) = \begin{cases} \mathcal{X}_0(i, j)^{-1} & \text{if } i + j \in 2\mathbb{Z}, \\ \mathcal{X}_0(i, j) \frac{(1+\mathcal{X}_0(i, j+1))(1+\mathcal{X}_0(i, j-1))}{(1+\mathcal{X}_0(i+1, j))^{-1}(1+\mathcal{X}_0(i-1, j))^{-1}} & \text{if } i + j \in 2\mathbb{Z} + 1. \end{cases} \quad (8.4)$$

Subsequently applying the sequence of mutations that takes S_1 to $S_2 = S_0$ yields the cluster variables

$$\mathcal{X}_2(i, j) = \begin{cases} \mathcal{X}_1(i, j)^{-1} & \text{if } i + j \in 2\mathbb{Z} + 1, \\ \mathcal{X}_1(i, j) \frac{(1+\mathcal{X}_1(i+1, j))(1+\mathcal{X}_1(i-1, j))}{(1+\mathcal{X}_1(i, j+1))^{-1}(1+\mathcal{X}_1(i, j-1))^{-1}} & \text{if } i + j \in 2\mathbb{Z}. \end{cases} \quad (8.5)$$

For $k \in 2\mathbb{Z} + 1$, \mathcal{X}_{k+1} is determined from \mathcal{X}_k by the same formula as \mathcal{X}_1 is determined from \mathcal{X}_0 . For $k \in 2\mathbb{Z}$, \mathcal{X}_{k+1} is determined from \mathcal{X}_k by the same formula as \mathcal{X}_2 is determined from \mathcal{X}_1 . Therefore these formulas determine a sequence $(\mathcal{X}_k)_{k \in \mathbb{N}}$. Moreover, for $k \in 2\mathbb{Z} + 1$, \mathcal{X}_{k-1} is determined from \mathcal{X}_k by the same formula as \mathcal{X}_2 is determined from \mathcal{X}_1 . For $k \in 2\mathbb{Z}$, \mathcal{X}_{k-1} is determined from \mathcal{X}_k by the same formula as \mathcal{X}_1 is determined from \mathcal{X}_0 . Therefore, we actually get a sequence $(\mathcal{X}_k)_{k \in \mathbb{Z}}$.

Next, consider a function $\bar{\mathcal{X}} : \mathcal{L} \rightarrow \mathbb{C}$ defined from the sequence $(\mathcal{X}_k)_{k \in \mathbb{Z}}$ as defined above, such that

$$\bar{\mathcal{X}}(i, j, k) = \mathcal{X}_{k+1}(i, j). \quad (8.6)$$

It is a straight-forward calculation to show that $\bar{\mathcal{X}}$ is a Y-system as defined in Definition 5.1. Moreover, any Y-system defines a unique sequence $(\mathcal{X}_k)_{k \in \mathbb{Z}}$ related by square grid cluster mutations. Therefore, Y-systems and sequences of cluster variables on square grid quivers are equivalent.

Remark 8.1. Since the square grid quiver is a planar quiver with bipartite dual, there is also an identification with the *dimer model* [Ken03]. The dimer model is a statistical model for the weighted counting of perfect matchings on a graph. Each cluster mutation corresponds to a local change of the combinatorics of the graph that does not change the dimer partition function. Therefore, dimer partition functions occur naturally as invariants of Miquel dynamics, see [Aff21, KLRR22, Aff23, AdTM22].

9 X-variables for harmonic embeddings

For the treatment of harmonic embeddings we use more general combinatorics than \mathbb{Z}^2 , while abandoning the lattice perspective for the moment. We explain at the end of the section how the A_3 lattice perspective is recovered in the \mathbb{Z}^2 case.

A quad-graph is a planar graph G such that each face is a quad. An *h-embedding* is a map $h : E(G) \rightarrow \mathbb{C}$ such that the image of each quad is a non-degenerate rectangle, and such that the sides of no two rectangles intersect except at their endpoints.

An orthodiagonal quad is a quad such that the diagonals are orthogonal. An *orthodiagonal embedding* is an embedding $o : V(G) \rightarrow \mathbb{C}$ such that the image of each quad is a non-degenerate orthodiagonal quad, and such that the sides of no two rectangles intersect except at their endpoints. To each orthodiagonal embedding o we obtain a unique *h-embedding* via $h(v, v') = \frac{1}{2}(o(v) + o(v'))$. This operation can be reversed assuming we

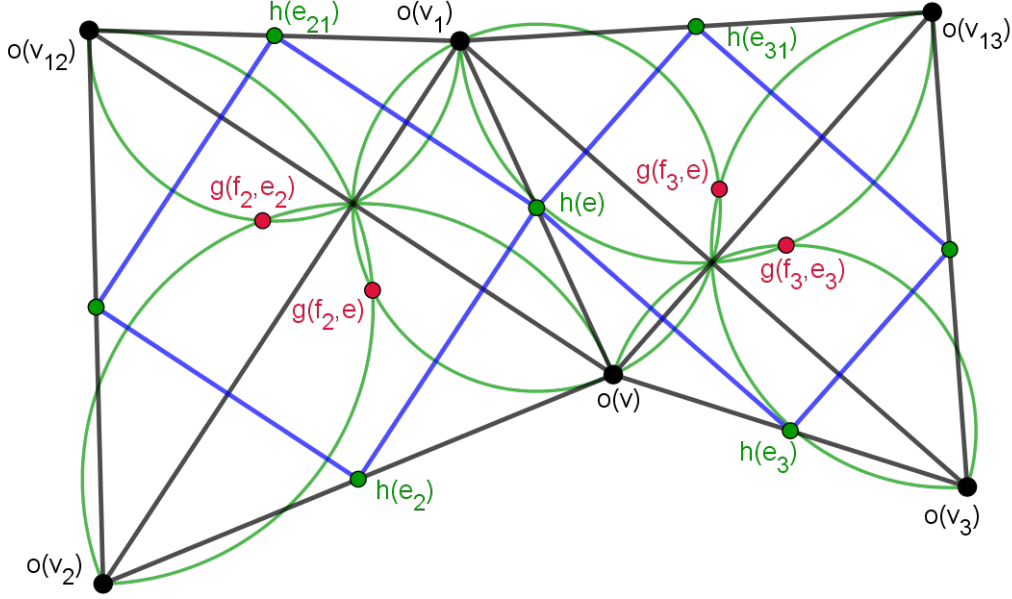


Figure 13. Two adjacent orthodiagonal quads with labeling.

know $o(v_0)$ for some $v_0 \in V(G)$, since we obtain $o(v)$ as a reflection of $o(v')$ about $h(v, v')$ for all $(v, v') \in E(G)$. However, if we choose $o(v_0)$ differently it is not guaranteed that o will be an embedding. In the following, we assume that both o and h are embeddings.

The relation between h -embeddings, orthodiagonal embeddings and h -embeddings is due to [KLR22]. In particular, the restriction of o to half the vertices may be considered a *harmonic embedding*.

We also introduce a map of circles c defined on the edges $E(G)$, such that $c(v, v')$ has center $h(v, v')$ and contains both $o(v)$ and $o(v')$. As a result, we see that an h -embedding is a special case of a conical net. Let $e \in E(G)$ be an edge and consider a labeling as in Figure 13. We define the Y -variables $E(G) \rightarrow \mathbb{R}$ via

$$Y(e) = -\frac{(h(e_2) - h(e))(h(e_{31}) - h(e))}{(h(e_{21}) - h(e))(h(e_3) - h(e))}. \quad (9.1)$$

For an orthodiagonal map o , let us denote by $d(f) \in \mathbb{C}$ the diagonal intersection point of f . Let us introduce two extra points per quad which we call *focal-points*. For each choice of a face $f \in F(G)$ and opposite edges e, e' in f , let $g(f, e) \in \mathbb{C}$ be the intersection point of $c(e)$ and $c(e')$ which is not $d(f)$. We will use an explicit formula for the focal points as given in the next lemma.

Lemma 9.1. With the labeling of Figure 13 holds

$$g(f_2, e) = \frac{o(v_1)o(v_{12}) - o(v)o(v_2)}{o(v_1) + o(v_{12}) - o(v) - o(v_2)}, \quad (9.2)$$

Proof. It is not hard to check that this formula is invariant under translations and scale-rotations. Therefore we may assume that the diagonal intersection point $d(f_2)$ is at 0 and that the diagonals are axis-aligned, specifically we assume that

$$\bar{o}(v) = o(v), \quad \bar{o}(v_1) = -o(v_1), \quad \bar{o}(v_{12}) = o(v_{12}), \quad \bar{o}(v_2) = -o(v_2). \quad (9.3)$$

The point $g(f_2, e)$ is the reflection of $d(f_2)$ about the line spanned by $h(e)$ and $h(e_1^2)$, therefore

$$g(f_2, e) = h(e) - \overline{h(e)} \frac{h(e_1^2) - h(e)}{h(e_1^2) - \overline{h(e)}} = \frac{h(e)\overline{h(e_1^2)} - \overline{h(e)}h(e_1^2)}{h(e_1^2) - \overline{h(e)}}. \quad (9.4)$$

Expressing h via o then yields

$$g(f_2, e) = \frac{1}{2} \frac{(o(v) + o(v_1))(\bar{o}(v_2) + \bar{o}(v_{12})) - (\bar{o}(v) + \bar{o}(v_1))(o(v_2) + o(v_{12}))}{\bar{o}(v_2) + \bar{o}(v_{12}) - \bar{o}(v) - \bar{o}(v_1)}. \quad (9.5)$$

Using the assumptions in Equation (9.3) in the last formula yields the claim. \square

Next, we introduce X -variables $X : E(G) \rightarrow \mathbb{R}$ for orthodiagonal maps. Let $e \in E(G)$ be an edge and consider a labeling as in Figure 13. Then we define

$$X(e) := -\text{cr}(o(v), g(f_2, e), o(v_1), g(f_3, e)). \quad (9.6)$$

Theorem 9.2. The two variables X, Y coincide, that is $X(e) = Y(e)$ for all $e \in E(G)$.

Proof. Using Lemma 9.1 and a quick calculation shows that

$$\frac{h(e) - h(e_{21})}{h(e) - h(e_2)} = \frac{o(v) - o(v_{12})}{o(v_1) - o(v_2)} = -\frac{o(v_1) - g(f_2, e)}{g(f_2, e) - o(v)}. \quad (9.7)$$

Each Y -variable is defined by two ratios of the kind on the left most side, while each corresponding X -variable is defined by two ratios of the kind on the right most side, which proves the claim. \square

The Y -variables were considered as cluster variables in [KLRR22], which were shown to be in the so called *resistor subvariety*, see [GK13]. Since Y - and X -variables coincide, the X -variables are also in the resistor subvariety, and they satisfy the same recursion equations as the Y -variables for the so called *cube-flip*.

A difference between Y -variables and X -variables is that the X -variables are inherently Möbius invariant. Thus it is possible to apply a Möbius transformation M to the circles c defined on the edges of G . This yields a new circle pattern for which we may define the X -variables analogously to before, and the X -variables of $M(c)$ will agree with the X -variables of c . However, the resulting circle configuration does not define an h -embedding anymore. It would be interesting to understand the set of maps that are obtained by applying Möbius transformations to the circles of an h -embedding in more detail, and whether this is in some sense a meaningful Möbius generalization of harmonic embeddings.

If the quad-graph G is \mathbb{Z}^2 , then $E(G) \simeq \mathbb{Z}^2$ as well. We may choose the identification in such a way that the black faces of \mathbb{Z}^2 correspond to the vertices of G and the white faces of \mathbb{Z}^2 correspond to the faces of \mathbb{Z}^2 . In this case, the X -variables we defined for h -embeddings are the X^\bullet -variables. Any circle pattern such that the circle centers around each white face constitute a rectangle and such that the edges do not cross is an h -embedding. However, we do not know whether these are all circle patterns such that X^\bullet - and Y -variables coincide.

Question 9.3. Is there a geometric characterization of all circle patterns or Miquel maps that satisfy $X^\bullet = Y$?

Remark 9.4. In fact, as outlined in the thesis [Aff23], the point of h -embeddings defined on minimal quad-graphs and all their cube-flips may be understood as being a dSKP map on the A_{2n-1} lattice, where n is the number of strips in the quad-graph. The points of an h -embedding h , the orthodiagonal map o , its focal points and all their cube-flips are a dSKP map on the A_{2n} lattice. In the language of cluster algebras: for some boundary data of h together with all data of o , there exists a sequence of mutations that transforms this into all of h and some boundary data of o , and vice versa.

Remark 9.5. In the case of s -embeddings (see [Che18]) an analogous construction as in the case of h -embeddings is possible. In particular, by including the incircle centers of an s -embedding one obtains a t -embedding, which is accompanied by a circle pattern. Again, it is possible to associate to that circle pattern X -variables that have the same combinatorics as the Y -variables and are expressed by certain real cross- and multi-ratios. However, we do not see any immediate relation between the X - and Y -variables of s -embeddings, nor are the X -variables of s -embeddings in the Ising subvariety. The only thing we claim here without proof is that the X -variables of s -embeddings satisfy the hexahedron recurrence (see [KP16] for a definition of the hexahedron recurrence).

References

- [ABS12] Vsevolod E. Adler, Alexander I. Bobenko, and Yuri B. Suris. Classification of Integrable Discrete Equations of Octahedron Type. *International Mathematics Research Notices*, 2012(8):1822–1889, 01 2012. 3, 5, 11, 12, 14
- [AdTM22] Niklas C. Affolter, Béatrice de Tilière, and Paul Melotti. The Schwarzian octahedron recurrence (dSKP equation) II: geometric systems, 2022. arXiv preprint, 2305.02212. 10, 21
- [Aff21] Niklas C. Affolter. Miquel dynamics, Clifford lattices and the Dimer model. *Letters in Mathematical Physics*, 111:1–23, 2021. 3, 5, 9, 11, 16, 21
- [Aff23] Niklas C. Affolter. Discrete Differential Geometry and Cluster Algebras via TCD maps, 2023. PhD thesis, arXiv:2305.02212. 5, 21, 24
- [BdT12] Cédric Boutillier and Béatrice de Tilière. Statistical mechanics on isoradial graphs. In *Probability in Complex Physical Systems*, pages 491–512, Berlin, Heidelberg, 2012. Springer Berlin Heidelberg. 16
- [BMS05] Alexander I. Bobenko, Christian Mercat, and Yuri B. Suris. Linear and non-linear theories of discrete analytic functions. Integrable structure and isomonodromic Green’s function. *Journal für die reine und angewandte Mathematik*, 2005(583):117–161, 2005. 5, 16
- [BS08] Alexander I. Bobenko and Yuri B. Suris. *Discrete Differential Geometry: Integrable Structure*. Graduate studies in mathematics. Birkhäuser, 2008. 5
- [Che18] Dmitry Chelkak. Planar Ising model at criticality: state-of-the-art and perspectives. In *Proceedings of the International Congress of Mathematicians—Rio de Janeiro 2018. Vol. IV. Invited lectures*, pages 2801–2828. World Sci. Publ., Hackensack, NJ, 2018. 6, 24

- [CLR23] Dmitry Chelkak, Benoît Laslier, and Marianna Russkikh. Dimer model and holomorphic functions on t-embeddings of planar graphs. *Proceedings of the London Mathematical Society*, 126(5):1656–1739, 2023. 3
- [DN91] Irene Ya. Dorfman and Frank W. Nijhoff. On a (2+1)-dimensional version of the Krichever-Novikov equation. *Physics Letters A*, 157(2):107–112, 1991. 3
- [FZ01] Sergey Fomin and Andrei Zelevinsky. Cluster algebras I: Foundations. *Journal of the American Mathematical Society*, 15, 05 2001. 4, 20
- [GK13] Alexander B. Goncharov and Richard Kenyon. Dimers and cluster integrable systems. *Annales scientifiques de l'École Normale Supérieure*, 46(5):747–813, 2013. 23
- [Gli11] Max Glick. The pentagram map and Y-patterns. *Advances in Mathematics*, 227(2):1019 – 1045, 2011. 5
- [GR17] Max Glick and Dylan Rupel. Introduction to Cluster Algebras, 07 2017. Notes for lecture at ASIDE conference 2016. 20
- [Ken03] Richard W. Kenyon. An introduction to the dimer model. In *Lecture notes from a minicourse given at the ICTP in May 2002.*, 2003. 21
- [KLRR22] Richard W. Kenyon, Wai Yeung Lam, Sanjay Ramassamy, and Marianna Russkikh. Dimers and Circle patterns. *Annales Scientifiques de l'École Normale Supérieure*, 55(3):863–901, 2022. 3, 5, 6, 9, 11, 16, 21, 22, 23
- [KNS11] Atsuo Kuniba, Tomoki Nakanishi, and Junji Suzuki. T-systems and Y-systems in integrable systems*. *Journal of Physics A: Mathematical and Theoretical*, 44(10):103001, feb 2011. 4, 11
- [KP16] Richard W. Kenyon and Robin Pemantle. Double-dimers, the Ising model and the hexahedron recurrence. *Journal of Combinatorial Theory, Series A*, 137:27 – 63, 2016. 24
- [KS02] Boris G. Konopelchenko and Wolfgang K. Schief. Menelaus' theorem, Clifford configurations and inversive geometry of the Schwarzian KP hierarchy. *Journal of Physics A: Mathematical and General*, 35(29):6125–6144, 07 2002. 3, 5, 10
- [KS04] Richard W. Kenyon and Scott Sheffield. Dimers, tilings and trees. *Journal of Combinatorial Theory, Series B*, 92(2):295 – 317, 2004. Special Issue Dedicated to Professor W.T. Tutte. 5
- [Miq38] Auguste Miquel. Théorèmes sur les intersections des cercles et des sphères. *J. Math. Pures Appl.*, pages 517–522, 1838. 2
- [Mü15] Christian Müller. Planar discrete isothermic nets of conical type. *Beiträge zur Algebra und Geometrie / Contributions to Algebra and Geometry*, 57, 06 2015. 2
- [NCWQ84] Frank W. Nijhoff, Hans W. Capel, Gerlof L. Wiersma, and G. Reinout W. Quispel. Bäcklund transformations and three-dimensional lattice equations. *Physics Letters A*, 105(6):267–272, 1984. 3

- [NS97] Jonathan J. C. Nimmo and Wolfgang K. Schief. Superposition principles associated with the Moutard transformation: an integrable discretization of a $(2+1)$ -dimensional sine-Gordon system. *Proceedings of the Royal Society London A*, 453:255 – 279, 1997. 16
- [Ram18] Sanjay Ramassamy. Miquel Dynamics for Circle Patterns. *International Mathematics Research Notices*, 2020(3):813–852, 03 2018. 2
- [Zam91] Alexander B. Zamolodchikov. On the thermodynamic Bethe ansatz equations for reflectionless ADE scattering theories. *Physics Letters B*, 253(3):391–394, 1991. 11